Photosensitivity and thermal stability of UV-induced fiber Bragg gratings in phosphate glass fibers

Lingyun Xiong,[1,*] Peter Hofmann,[2] Axel Schülzgen,[2] N. Peyghambarian,[3] and Jacques Albert[1]

[1]*Department of Electronics, Carleton University, 1125 Colonel By Drive, Ottawa, Ontario K1S 5B6, Canada*
[2]*College of Optics and Photonics, CREOL, University of Central Florida, Orlando, Florida 32816, USA*
[3]*College of Optical Sciences, University of Arizona, Tucson, Arizona 85721, USA*
[*]*lxiong@doe.carleton.ca*

Abstract: The photosensitivity of highly Er/Yb doped and undoped phosphate glass fibers is characterized under irradiation with intense pulsed 193 nm light from an ArF excimer laser through a phase mask. The ultraviolet photosensitivity of the active fibers is shown to be roughly half that of the passive fibers. We also demonstrate that the strong growth of the fiber Bragg grating reflectivity observed upon heating at temperatures between 100 – 250 °C is directly related to the UV irradiation time, but not to the size of the index modulation of the seed grating or even to the fiber type (Er/Yb doped or undoped). The conditions to reliably obtain final index modulations amplitudes between 5 and 10×10^{-5} are given.

OCIS codes: (060.3735) Fiber Bragg gratings; (060.2290) Fiber materials; (060.3738) Fiber Bragg gratings, photosensitivity; (120.6810) Thermal effects.

References and links

1. P. Laporta, S. Taccheo, S. Longhi, O. Svelto, and C. Svelto, "Erbium–ytterbium microlasers: optical properties and lasing characteristics," Opt. Mater. **11**(2-3), 269–288 (1999).
2. L. Fletcher, J. Witcher, N. Troy, S. T. Reis, R. K. Brow, R. M. Vazquez, R. Osellame, and D. M. Krol, "Femtosecond laser writing of waveguides in zinc phosphate glasses," Opt. Mater. Express **1**(5), 845–855 (2011).
3. D. Grobnic, S. J. Mihailov, R. B. Walker, C. W. Smelser, C. Lafond, and A. Croteau, "Bragg gratings made with a femtosecond laser in heavily doped Er–Yb phosphate glass fiber," IEEE Photon. Technol. Lett. **19**(12), 943–945 (2007).
4. M. Sozzi, A. Rahman, and S. Pissadakis, "Non-monotonous refractive index changes recorded in a phosphate glass optical fibre using 248nm, 500fs laser radiation," Opt. Mater. Express **1**(1), 121 (2011).
5. P. Hofmann, C. Voigtlander, S. Nolte, N. Peyghambarian, and A. Schülzgen, "550-mW output power from a narrow linewidth all-phosphate fiber laser," J. Lightwave Technol. **31**(5), 756–760 (2013).
6. J. Albert, A. Schülzgen, V. L. Temyanko, S. Honkanen, and N. Peyghambarian, "Strong Bragg gratings in phosphate glass single mode fiber," Appl. Phys. Lett. **89**(10), 101127 (2006).
7. R. M. Rogojan, A. Schülzgen, N. Peyghambarian, A. Laronche, and J. Albert, "Photo-thermal gratings in Er^{3+}/Yb^{3+}-doped core phosphate glass single mode fibers," in *Bragg Gratings, Photosensitivity, and Poling in Glass Waveguides* (OSA, 2007), p. BTuC3.
8. L. Xiong, P. Hofmann, A. Schülzgen, N. Peyghambarian, and J. Albert, "Photo-thermal growth of unsaturated and saturated Bragg gratings in phosphate glass fibers," in *Bragg Gratings, Photosensitivity, and Poling in Glass Waveguides* (OSA, 2010), p. BTuB1.
9. A. Schülzgen, L. Li, D. Nguyen, Ch. Spiegelberg, R. M. Rogojan, A. Laronche, J. Albert, and N. Peyghambarian, "Distributed feedback fiber laser pumped by multimode laser diodes," Opt. Lett. **33**(6), 614–616 (2008).
10. L. Li, A. Schülzgen, X. Zhu, J. V. Moloney, J. Albert, and N. Peyghambarian, "1 W tunable dual-wavelength emission from cascaded distributed feedback fiber lasers," Appl. Phys. Lett. **92**(5), 051111 (2008).
11. A. Hidayat, Q. Wang, P. Niay, M. Douay, B. Poumellec, F. Kherbouche, and I. Riant, "Temperature-induced reversible changes in the spectral characteristics of fiber Bragg gratings," Appl. Opt. **40**(16), 2632–2642 (2001).
12. K. Seneschal, F. Smektala, B. Bureau, M. Le Floch, S. Jiang, T. Luo, J. Lucas, and N. Peyghambarian, "Properties and structure of high erbium doped phosphate glass for short optical fibers amplifiers," Mater. Res. Bull. **40**(9), 1433–1442 (2005).
13. S. Bandyopadhyay, J. Canning, M. Stevenson, and K. Cook, "Ultrahigh-temperature regenerated gratings in boron-codoped germanosilicate optical fiber using 193 nm," Opt. Lett. **33**(16), 1917–1919 (2008).

#211551 - $15.00 USD Received 1 May 2014; revised 11 Jun 2014; accepted 11 Jun 2014; published 23 Jun 2014

14. D. J. Little, M. Ams, P. Dekker, G. D. Marshall, and M. J. Withford, "Mechanism of femtosecond-laser induced refractive index change in phosphate glass under a low repetition-rate regime," J. Appl. Phys. **108**(3), 033110 (2010).
15. S. Gross, M. Ams, G. Palmer, C. T. Miese, R. J. Williams, G. D. Marshall, A. Fuerbach, D. G. Lancaster, H. Ebendorff-Heidepriem, and M. J. Withford, "Ultrafast laser inscription in soft glasses: a comparative study of athermal and thermal processing regimes for guided wave optics," Int. J. Appl. Glas. Sci. **3**(4), 332–348 (2012).
16. R. Kashyap, *Fiber Bragg Gratings*, 2nd edition (Academic Press, 2009).
17. S. Yliniemi, S. Honkanen, A. Ianoul, A. Laronche, and J. Albert, "Photosensitivity and volume gratings in phosphate glasses for rare-earth-doped ion-exchanged optical waveguide lasers," J. Opt. Soc. Am. B **23**(12), 2470–2478 (2006).
18. D. Ehrt, P. Ebeling, and U. Natura, "UV Transmission and radiation-induced defects in phosphate and fluoride–phosphate glasses," J. Non-Cryst. Solids **263–264**, 240–250 (2000).
19. L. Xiong, P. Hofmann, A. Schülzgen, N. Peyghambarian, and J. Albert, "Deep UV-induced near-infrared photodarkening of Er/Yb-doped and undoped phosphate fibers," Opt. Lett. **38**(20), 4193–4196 (2013).
20. J. Albert, "Permanent photoinduced changes for bragg gratings in silicate glass waveguides and fibers," MRS Bull. **23**, 36–42 (1998).

1. Introduction

Rare-earth-doped phosphate glass (without silica) is an important medium for high power amplifiers and compact fiber lasers because of the higher solubility of rare-earth elements relative to silica glass [1]. However, the lack of conventional photosensitivity in phosphate glass fibers used to prevent the integration of UV-written intra-fiber gratings into the laser cavity. One alternative way to inscribe gratings in phosphate glass is to resort to high energy femtosecond lasers. With the use of femtosecond laser at wavelengths of 248 nm or 800 nm, laser inscribed waveguides structure in bulk glasses and even strong Bragg gratings in phosphate fibers have been fabricated [2–5]. However, it is still of fundamental interest to investigate the photosensitivity of phosphate fibers to UV excimer lasers. In recent previous work, it was demonstrated that the direct writing of gratings in both undoped and Er/Yb doped (hereafter referred to as "passive" and "active") phosphate glass fibers was possible using an ArF excimer laser [6,7], and further shown that the grating index modulation in phosphate glass fibers can be strengthened by heating the gratings to temperatures between 100 and 250 °C [8]. This kind of photo-thermal process allows the formation of gratings with reflectivity above 90% and the fabrication of compact distributed feedback (DFB) lasers in active phosphate glass fibers [9,10].

In this paper, we systematically investigate the grating fabrication to determine under which conditions thermal growth is achievable by thermal annealing of seed Bragg gratings in passive and active phosphate glass fibers. In particular, we show that the UV irradiation time is the critical parameter in achieving strong photo-thermal growth, regardless of the index modulation amplitude or contrast of the seed grating, and regardless of the core dopants. It is also shown that for the first part of the process (the UV induced index change), the photosensitivity of the passive fibers is about two times larger than that of the active fibers.

2. UV-induced fiber Bragg gratings fabrication

Grating fabrication experiments were performed on two types of fiber samples: phosphate fiber with Er/Yb doped core (Fiber A, A for active) and undoped phosphate fiber (Fiber P, P for passive). The Er/Yb doped fiber has a highly doped core with 1 wt% Er_2O_3 and 8 wt% Yb_2O_3, while the undoped fiber is free of Er/Yb dopants in the core. Phosphate fibers were prepared as 5-cm long samples, and were spliced to standard telecommunication (CORNING SMF 28) fiber pigtails. Bragg gratings were written in both types of phosphate glass fibers by using intense UV irradiation from a pulsed excimer laser (PulseMaster 840 series from GSI Lumonics). Operating at wavelength of 193 nm with a gas mixture of ArF, the laser delivered pulses with durations of about 20 ns at a repetition rate of 50 Hz. After passing through beam shaping elements such as apertures and a beam expander, the UV laser beam was focused through a cylindrical lens along the fiber axis to generate a high intensity region with a fluence per pulse of ~45 mJ/cm^2. A phase mask with a period of 988.4 nm is placed just in front of the fiber samples to generate fringe patterns over a length of 2 cm on the fiber. During the grating inscription, the grating transmission spectrum was monitored and recorded

#211551 - $15.00 USD Received 1 May 2014; revised 11 Jun 2014; accepted 11 Jun 2014; published 23 Jun 2014

continually by launching broadband light in the fiber and measuring the transmitted light with an optical spectrum analyzer. The growth evolution of the average refractive index change and the refractive index modulation of the FBG can be calculated from the measured position and amplitude of the reflection resonance in the transmission spectra. For a uniform FBG, the average refractive index change Δn_{avg} and refractive index modulation Δn_{mod} are determined by:

$$\Delta n_{avg} = \frac{\Delta \lambda_B}{2\Lambda\eta} \tag{1}$$

$$\Delta n_{mod} = \tanh^{-1}(\sqrt{R})\frac{\lambda_B}{\pi L\eta} \tag{2}$$

where λ_B is the Bragg wavelength, $\Delta\lambda_B$ is the Bragg wavelength shift during the grating fabrication process, R is the power reflectivity at the Bragg wavelength, Λ is the grating period, L is the grating length, and the confinement factor η (equal to 0.75 here) is the fraction of total power of the fundamental mode confined in the fiber core area.

3. Experimental results and discussions

Figure 1 illustrates the growth of the average refractive index change Δn_{avg} and refractive index modulation Δn_{mod} during grating fabrication on both passive and active phosphate fibers. For the sake of easy comparison, the Δn_{avg} of passive and active fiber samples is plotted side by side with the same scale. The Δn_{mod} for both fibers is also presented with an enlarged scale compared to Δn_{avg}, in order to show the details of growth pattern. Gratings P1-P4 and A1-A4 were fabricated with the same grating fabrication setup, aligned to generate strong grating index modulations. Gratings P5-P8 were fabricated with an earlier setup that led to premature saturation of the fringe contrast and hence of the Δn_{mod} as reported earlier [8].

Except for Δn_{mod} of samples P5 and P6, the growth curves of all the samples in each graph follow the same stretched exponential function (calculated from samples P1-P3 and A1-A3 only), within the +/–95% prediction band limits. Remaining small differences in the grating growth patterns within each fiber type can be attributed to irradiation conditions from the excimer laser, such as pulse energy variations, UV beam spatial stability, and imperfect homogeneity of these laboratory-made phosphate fiber samples.

The refractive index changes follow nearly monotonic (again, apart from P5-P6) growth curves without showing signs of saturation for long UV irradiation times (up to ~1100 s). Small oscillations in almost all the growth curves are likely due to a small multimode interference (MMI) effect arising from the excitation of some lower order cladding modes within the short length of phosphate fibers that are spliced between the SMF pigtails. The MMI effect not only introduces small quasi-periodic oscillations in the spectral baseline of the measured FBG transmission spectra, but also the amount of light that recombines in the core at the downstream splice at the wavelength of the grating. These two effects combine to change periodically both the amplitude and position of the Bragg resonance, but in a way that does not obscure the main trends of the UV-induced refractive index changes. The sudden drop of Δn_{avg} near the end of the curves on Fig. 1 indicates the point where the UV irradiation is switched off. This is commonly observed in FBGs fabrication because the fiber temperature increases slightly (by about 6°C here, based on a measured $d\lambda/dT$ of 11 pm/°C) during irradiation with high average power UV sources. In all sections below, the value of Δn_{avg} that are reported are the "cold" ones, as they reflect the actual values at room temperature. Unfortunately, there is no rigorous way to remove the temperature contribution from the Δn_{avg} growth curves obtained in real time but since it affects all fibers the same way, we felt it was still interesting to plot the comparative growth dynamics in Fig. 1.

#211551 - $15.00 USD Received 1 May 2014; revised 11 Jun 2014; accepted 11 Jun 2014; published 23 Jun 2014

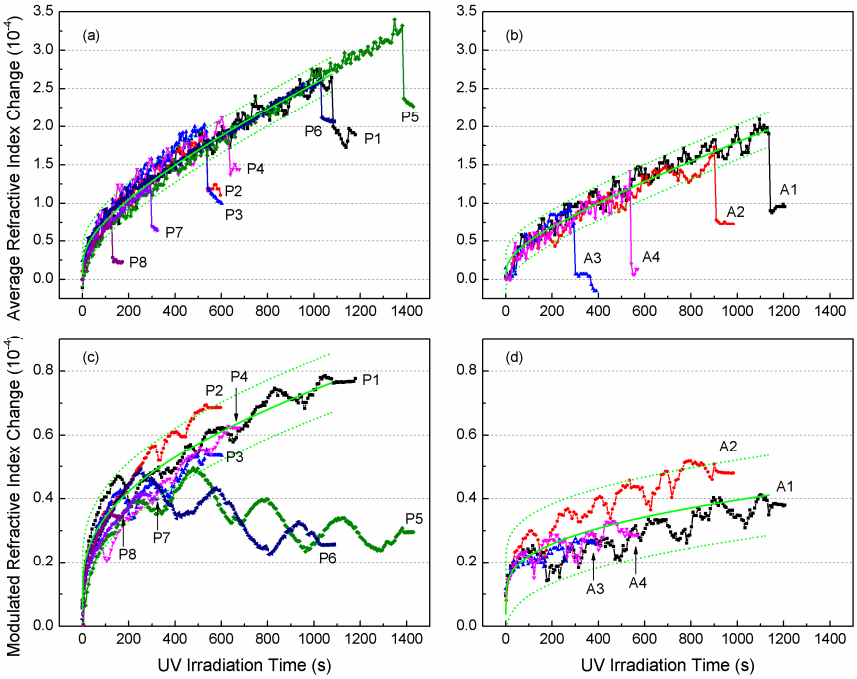

Fig. 1. Refractive index changes during fabrication of 2 cm-long gratings in passive and active phosphate fibers: (a) Δn_{avg} in passive fibers (samples P1-P8), (b) Δn_{avg} in active fibers (samples A1-A4), (c) Δn_{mod} in passive fibers and (d) Δn_{mod} in active fibers. Green solid and dash lines are fitted stretched exponential curves and their respective 95% prediction bands.

The first clear observation from Fig. 1 is that the passive phosphate fiber samples exhibit larger UV photosensitivity than the active fiber samples, evidenced by higher refractive index change in terms of both Δn_{avg} and Δn_{mod}: the passive fibers reach Δn_{avg} of ~2.0×10^{-4}, while the active fibers show lower Δn_{avg} of ~9.6×10^{-5}. For the grating refractive index modulation, the passive fibers reach Δn_{mod} of ~7.6×10^{-5} (corresponding to grating transmission notch depth of ~14.3 dB), and the active fibers only achieve a maximum Δn_{mod} of ~4.8×10^{-5} (corresponding to grating transmission notch depth of ~7.2 dB). We note that the grating fringe contrast ratios ($\Delta n_{mod}/\Delta n_{avg}$) are only 0.38 and 0.40 for passive and active phosphate fibers respectively, compared to 0.67 for silica fibers (SMF28) with low-Ge doped cores that were exposed in the same setup. The difference could be due to different mechanisms for the UV-induced Δn_{avg} and Δn_{mod}.

Figure 1 also shows that the Δn_{mod} of gratings P5-P6 stops growing between 300 and 500 seconds of irradiation, while the Δn_{avg} follows the general trend. This indicates loss of contrast, which may be attributed to instabilities in the beam or in the mechanical set-up. Surprisingly, it will be shown below that this loss of contrast during irradiation had little effect on the subsequent thermal growth of Δn_{mod}.

To investigate the thermally induced growth dynamics and the thermal stability of UV-induced FBGs in phosphate fibers, both passive and active FBG samples were subjected to a step-isothermal annealing treatment at temperatures from 100 °C to 300 °C in steps of 50 °C. For each step of isothermal annealing, the gratings were held at the same temperature for a duration of about 9 days, after which gratings were cooled down to room temperature before the next annealing cycle. Figure 2 illustrates the thermal evolutions of the transmission notch depths of several representative gratings in both passive and active phosphate fibers. All gratings except sample P8 exhibit a growth of the transmission notch depth (i.e., Δn_{mod} increases) upon thermal annealing at temperatures of 100 - 250 °C. However, beyond that a thermal decay of the grating strengths begins when the annealing temperature is further

#211551 - $15.00 USD Received 1 May 2014; revised 11 Jun 2014; accepted 11 Jun 2014; published 23 Jun 2014

increased to 300 °C. The discontinuities in the curves correspond partly to a reversible grating strength change that occurs when the fibers are returned to room temperature between heating steps [11], and partly to a change in the interference pattern of the MMI due to the change in temperature. In order to minimize the impact of this artifact, an average between the measured notch depth values at the annealing temperature and at room temperature was used to calculate the final Δn_{mod} values (labeled in Fig. 2) at the end of the 250 °C step.

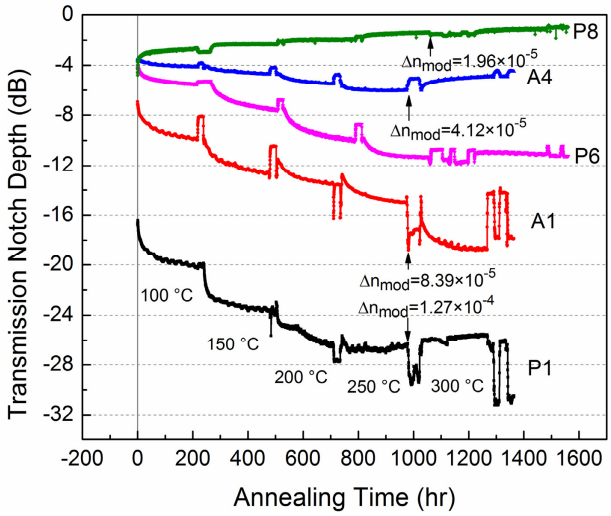

Fig. 2. Thermal evolution of the transmission notch depths for gratings in passive (P1, P6, P8) and active (A1, A4) phosphate fibers during step-wise annealing between 100 – 300 °C, in 50 °C steps for 9-11 days at each step and return to room temperature between steps. See text for further details.

Figure 3 shows the evolution of transmission spectra of one example grating P1 before and after each thermal annealing step. All spectra were measured at room temperature between heating steps. Clearly, UV induced gratings in phosphate glass fibers maintain excellent spectral quality from the initial seed grating and throughout the thermal growth process, accompanied by a blue shift due to the decay of Δn_{avg}. The linewidth of this 2-cm-long FBG increased from 0.09 nm to 0.19 nm as expected from the increase in grating strength.

Before exploring further the impact of thermal annealing on Δn_{mod}, its effect on Δn_{avg} is illustrated in Fig. 4. Those values are extracted from the wavelength shifts of the grating resonances measured at room temperature between each heating step. The thermally induced Δn_{avg} of all the samples is plotted relative to their pre-annealing (but post-irradiation) values. In order to facilitate comparisons between gratings, the as-written value of Δn_{avg} for each sample is included beside its label name. In contrast to the thermal behavior of Δn_{mod}, Δn_{avg} exhibits a thermal decay for all annealing cycles and fibers, even at the relatively low heating temperature of 100 °C. Furthermore, the thermal decay of Δn_{avg} is almost completely independent of its initial value (and hence the UV irradiation time), as all samples fabricated in the same type of fiber experience the same decay amount.

#211551 - $15.00 USD Received 1 May 2014; revised 11 Jun 2014; accepted 11 Jun 2014; published 23 Jun 2014

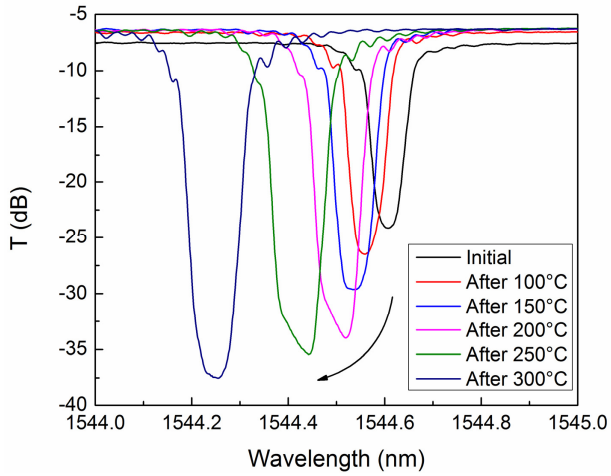

Fig. 3. Evolution of transmission spectra of grating P2 measured at room temperature, starting from the UV induced seed and after each thermal annealing step.

However, the thermal decay in the active fibers (with Er/Yb dopants) is smaller (by about 50%) than in passive fibers (this is the same ratio that was observed for the UV-induced growth in Fig. 1). It is interesting to note that the thermally induced decay of Δn_{avg} can be even larger than the Δn_{avg} increase induced during UV illumination. Therefore, the average core refractive indices of both types of phosphate fibers can be lower than their as-drawn values following irradiation and thermal processing. The total average decay of Δn_{avg} reached after thermal processing amounts to ~3.6×10^{-4} and ~1.4×10^{-4} in passive and active fibers, respectively. Separate experiments on similar fibers have been made where the annealing treatment was performed prior to the UV irradiation and have shown that the core index (as measured by the starting Bragg wavelength at low fluence) is unchanged from that of un-annealed fibers.

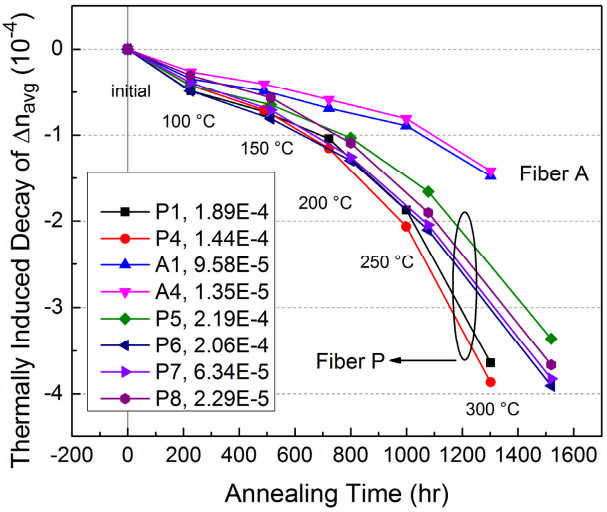

Fig. 4. Thermally induced decay of the average refractive index change Δn_{avg} relative to its initial value for gratings in passive and active phosphate glass fibers during the annealing described in the caption of Fig. 2. The initial absolute value of Δn_{avg} for each sample is included in the legend labels.

Finally, the thermally induced change of Δn_{mod} is plotted versus the UV irradiation time applied to inscribe the seed gratings in Fig. 5. The thermally induced changes of Δn_{mod}

#211551 - $15.00 USD Received 1 May 2014; revised 11 Jun 2014; accepted 11 Jun 2014; published 23 Jun 2014

presented here are the differences between Δn_{mod} after annealing at 250 °C and their respective values obtained just after UV-irradiation. The thermal decay observed at 300 °C is not considered here, as our investigation aims to find a recipe to maximize the thermal growth of Δn_{mod}. As shown in Fig. 5, there is a clear correlation between the thermally induced change of Δn_{mod} and the UV irradiation time that produced the seed gratings, despite of the differences in fiber types and grating fabrication setup alignments. The longer the fibers were exposed to UV irradiation, the larger the thermal growth that can be achieved to maximize Δn_{mod}. However, this occurs regardless of the starting value of Δn_{mod}, as evidenced by fibers P1, P5, and P6. It is also notable that this is the only result in which there is no observable difference between passive and active fibers. Also note, for irradiation times less than about 300 s, there is a decay of Δn_{mod} upon thermal annealing instead of a growth.

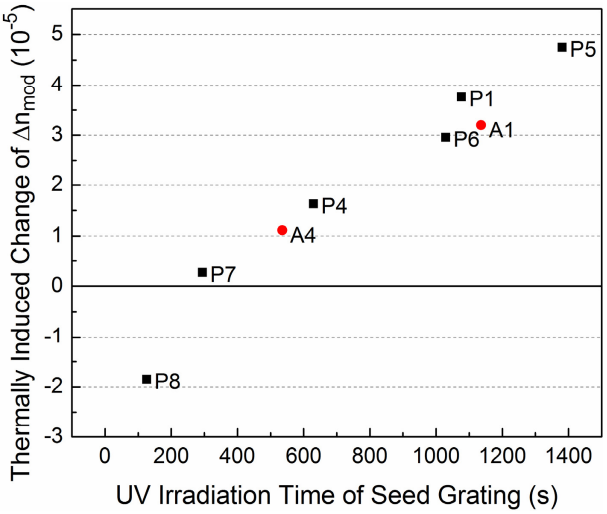

Fig. 5. Thermally induced change of refractive index modulation Δn_{mod} at the end of the 250 °C anneal step versus the UV irradiation time applied to produce the seed gratings.

While the UV photosensitivity observed here follows well established trends (stretched exponential monotonic growth and lesser growth when some additional absorption is present, as is the case of the active fibers), the thermal behavior of the gratings is completely anomalous. Normally, the reflectivity of UV-induced gratings (i.e. Δn_{mod}) decays with increasing temperature, in a range well below the glass transition temperature (T_g) (i.e. for annealing in the 100-300 °C range for silica fibers with a T_g above 1000 °C). Here, the opposite occurs at temperatures, up to 250 °C, that are quite close to the glass transition temperature of these glasses (~448 °C) [12]. Furthermore, while the decay of Δn_{avg} is expected, in the current case this decay is larger than the increase that was obtained during UV-irradiation.

These observations are also different from the behavior of regenerated gratings in hydrogenated silica glass fibers [13], in which Δn_{mod} shows a complete erasure followed by a regeneration upon annealing at ~900 °C. Here, Δn_{mod} exhibits monotonic growth without any erasure during heat treatment. The low T_g of phosphate glass, along with the very strong correlation between the total UV irradiation, the total amount of thermal decay of the average index, and the amount of observed thermal growth of Δn_{mod} indicate a complex photo-thermal process that may involve several index change mechanisms.

As mentioned earlier, there are few prior studies of the optical and structural properties of UV-irradiated phosphate glasses. However, several groups have used ultrafast laser techniques to permanently modify the refractive index of phosphate glasses, both for making gratings and to write waveguides in bulk samples [2–5,14,15]. These references also indicate that the photosensitivity of phosphate glass is indeed a complicated process which can even generate either positive or negative index changes depending on the glass composition and

#211551 - $15.00 USD Received 1 May 2014; revised 11 Jun 2014; accepted 11 Jun 2014; published 23 Jun 2014

laser irradiation conditions. As in the case of silica glasses [16], the photosensitivity of P-glass is thought to arise from two contributions: 1) a glass structural modification due to UV (or multiphoton) breaking of bonds in the glass network, and 2) the formation of color centers. Based on these findings, and the fact that ultrafast laser irradiation of glasses has similarities with lower intensity UV-irradiation as it relies on multiphoton effects to disrupt the electronic structure of glasses, the following phenomenological model is proposed to explain the results presented here. In this model (shown schematically in Fig. 6), and based on generally accepted theories for the photosensitivity of glasses, high-intensity UV irradiation in the bright fringes of the interference pattern used to fabricate the grating breaks some glass network bonds (P-O bonds in this case) and induces de-polymerization of the phosphate glass network [2,4,17]. In our case, the result is a glass densification which occurs from the collapse of the long chain structure into a shorter-range structure. Color centers are also created in the bright fringes, with a strong absorption at 630 nm that has been assigned to phosphorus oxygen hole center as well as shorter wavelength bands assigned to other P centers [18,19]. Both of these effects increase the refractive index in the bright fringes but while the color center contribution to the index increase occurs faster, it saturates at a low level, and is thermally unstable [20]. Some index increase also occurs between the bright fringes because the interference pattern resulting from the proximity phase mask technique is not perfect and does not have 100% modulation depth. It is also well established that structural effects tend to become more thermally stable during long irradiations as the glass network increasingly deforms from its initial state.

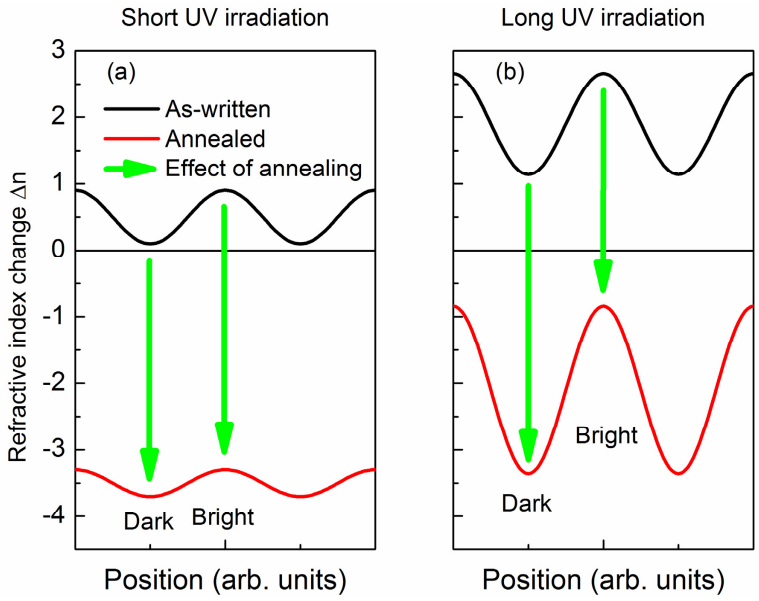

Fig. 6. Phenomenological model of photo-induced index change (black line), thermal annealing (green arrows) and final index changes (red line) for (a) short UV irradiation and (b) long UV irradiation. See text for details.

Based on these general considerations, our results can be explained in the following manner. UV irradiation increases the refractive index of the glass everywhere, but more strongly in the bright fringes. The result is an increase in the average index and in the index modulation, as observed in Fig. 1. Thermal processing erases quickly the color center contribution and the more thermally unstable part of the structural changes, i.e. the index decreases more quickly in the dark fringes than in the bright fringes, resulting in an increase in the index modulation, and the difference in the thermal decay rate is larger for gratings written for longer times. The only exception to the latter process is for the case of very short irradiations, where the index increase in the bright fringes is small and mostly due to color

#211551 - $15.00 USD Received 1 May 2014; revised 11 Jun 2014; accepted 11 Jun 2014; published 23 Jun 2014

centers and relatively unstable structural contributions, with little index change in the dark fringes. This leads to decay of the index modulation as well as of the average index (fiber P8). The main peculiarity of the P-glass system then becomes the fact that the negative shift of the average index during annealing is relatively independent of the irradiation time and appears to be larger than the amount of increase observed during the UV irradiation. We believe this to be due to the fact that the whole fiber (core and cladding) is somewhat photosensitive and therefore that the structural damage suffered during the irradiation allows the fiber to relax thermally towards a less dense state with lower average index during annealing. Micro-analysis of the physical state of the glass at various stages of processing will be required to confirm these hypotheses.

As a final comment, it is worth mentioning that it is quite a bit easier to achieve large refractive index modifications in many kinds of glasses and other materials with ultrafast laser irradiation [15]. However the current approach to achieve practically useful refractive index modulations in phosphate glasses from UV irradiation still has merit as it allows the writing of strong and thermally stable gratings with high spectral quality (Fig. 3) from conventional fiber and waveguide grating fabrication tools (excimer laser and phase mask).

4. Conclusion

In conclusion, a systematic investigation of the UV photosensitivity and thermal stability of gratings written by intense 193 nm irradiation in both undoped and Er/Yb doped phosphate glass fibers was performed. The conditions required to form a high reflectivity FBG in phosphate fibers through a combined photo-thermal process were determined: it basically consist of a prolonged UV irradiation (we used 20 minutes at 50 pulses per second and 46 mJ/cm^2 pulse fluence at the fiber) with some modulation of the UV light pattern to form a seed grating, followed by gradual heating up to 250 °C. These conditions, which are the same for undoped and doped fibers, were shown to lead to strong refractive index modulation with $\Delta n_{mod} \sim 1.3 \times 10^{-4}$ in undoped fibers and 8.4×10^{-5} in doped fibers. Further annealing at 300 °C reverses the process and induces the beginning of a decay in Δn_{mod}. Over the whole annealing process, a significant decay of the average core refractive index change Δn_{avg} is observed in all fibers at all annealing temperatures, leading to a net negative Δn_{avg} (up to -1×10^{-4}) relative to the value of as drawn core refractive indices. With regards to the long term thermal stability of these gratings, the fact that heating to 250 °C for as long as 9 days does not lead to Δn_{mod} decay is a very encouraging feature.

Acknowledgments

This work was supported by the Natural Sciences and Engineering Research Council of Canada, the Canada Research Chairs program, and the Center for Integrated Access Networks (CIAN), an NSF Engineering Research Center.

#211551 - $15.00 USD Received 1 May 2014; revised 11 Jun 2014; accepted 11 Jun 2014; published 23 Jun 2014